WEDNESDAY SLIDE CONFERENCE 2023-2024

Conference #6   27 September 2023

CASE I:

Signalment:
9-month-old female Saker Falcon, avian (*Falco cherrua*)

History:
A 9-month-old female Saker Falcon kept in a zoo had been showing signs of fatigue during training and loss of appetite for a few weeks, but her weight was stable. She was mainly fed mice and a change of food to quail and chicks improved her appetite. She died a few hours following her daily training, from which she returned breathless.

Gross Pathology:
The pericardial sac contained 1 to 2 ml of translucent light yellow gelatinous material. The heart and the liver showed slight cardiomegaly and hepatomegaly, respectively. A few epicardial petechiae were present on the ventral aspect of the heart. The peripheral connective tissues were turgid and moist (edema). The spleen was diffusely pale. The wall of the aortic arch was diffusely thickened; the inner surface was irregular, wrinkled, and yellow. Lungs showed several extensive, poorly demarcated dark red patches, interpreted as congestion and/or hemorrhages.

Laboratory Results:
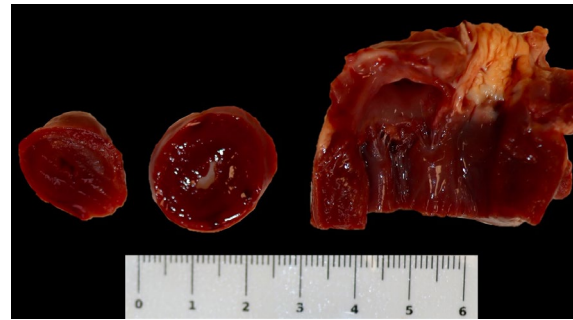PCR for highly pathogenic avian influenza virus (M gene): Negative.

Figure 1-1. Aorta, falcon. The wall of the aortic arch is diffusely thickened; the inner surface is irregular, wrinkled, and yellow. (*Photo courtesy of:* Laboratoire d'histopathologie animale, Vetagro Sup, campus vétérinaire, http://www.vetagro-sup.fr/)

Microscopic Description:

Brachiocephalic trunks, aortic arch, caudal aorta: The intima and subintimal media of arterial walls are diffusely and irregularly thickened by the accumulation of numerous large foamy cells, cholesterol clefts, large amorphous non-staining lipid deposits, and dense collagen (fibrosis). Occasionally, there are multifocal deposits of hyperbasophilic coarse granular material (mineralization) and cells located in lacunae within a chondroid matrix (chondroid metaplasia). The arterial lumen is often greatly reduced in diameter or almost absent (sub-occlusion). The adventitia is multifocally infiltrated by a small to moderate number of lymphocytes and plasma cells, and rare macrophages and Mott cells, which are occasionally accompanied by
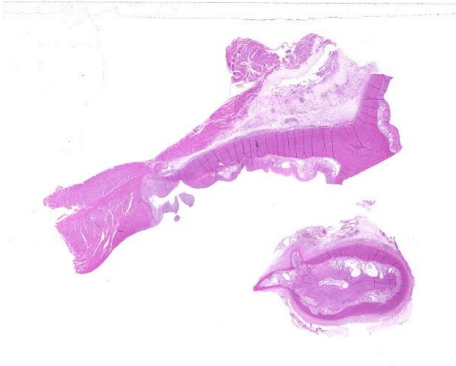
Figure 1-2. Aorta, falcon. A cross and longitudinal section of the aorta is presented for examination. The lumen is compromised and the tunica media is greatly expanded. (HE, 5X)

the accumulation of a variable amount of basophilic amorphous material (edema fluid). Within the aorta, lesions are visible in the vicinity of the heart, at the level of the aortic arch, and also in the abdominal region, near the adrenal glands. These lesions extend to the semi-lunar leaflets of the aortic valve. Early changes are seen in the intima of a pulmonary artery. Myxoid material is occasionally present between the smooth muscle fibers of the media.

Contributor's Morphologic Diagnosis:
Brachiocephalic trunks, aortic arch, caudal aorta: Atherosclerosis, multifocally extensive, severe, chronic, Saker Falcon, avian.

Contributor's Comment:

Although atherosclerosis is infrequent in domestic mammals, it is the most common cardiovascular disease found in birds of prey.[8] It is also common in other avian species, notably psittacine birds, but also chickens, finches, emus, and penguins.[21] It frequently occurs in non-human primates as well.[21] Furthermore, pigeons, Japanese quail, turkeys and chickens have been used as animal models of atherosclerosis for medical research.[6,19]

Atherosclerosis is a chronic inflammatory fibroproliferative disease that occurs in the arterial wall in response to endothelial injury. It results from an imbalance in lipid metabolism and an inappropriate immune response with accumulation of cholesterol-laden macrophages in the arterial wall. Atherosclerosis is one pattern of arteriosclerosis; other patterns include simple arteriosclerosis, Monckeberg sclerosis, and fibromuscular intimal hyperplasia.

In birds of prey, atherosclerosis primarily affects older captive individuals, but is reported in Brahminy kite (*Haliastur indus*) from 55 days of age and in other bird species (psittacine, raptors, waterfowl) from one year of age.[8,13,15] Female raptors and female psittacine birds have a higher risk of developing atherosclerosis than males, which may be due to the lipid metabolism involved in egg production.[3,12]

In humans, physical inactivity, obesity, unhealthy diet, hyperlipidemia, hypertension, and tobacco and high alcohol use are well-known risk factors for atherosclerosis, and the impact of exposure to these risk factors accumulates throughout life.[11] Obesity, lack of exercise, hypercholesterolemia, and a high-fat diet (cholesterol, saturated fatty acids) are also suspected risk factors for this disease in birds; however, captive conditions (nutrition, exercise) are not the determining factors in the development of this disease since atherosclerosis has been observed in wild individuals.[3,22] Genetic factors may also predispose animals to development of the condition, but in general, preventing obesity in captive birds and avoiding sudden weight loss in overweight individuals are recommended preventive measures.[8] A 2017 study also found an association between a diet con-
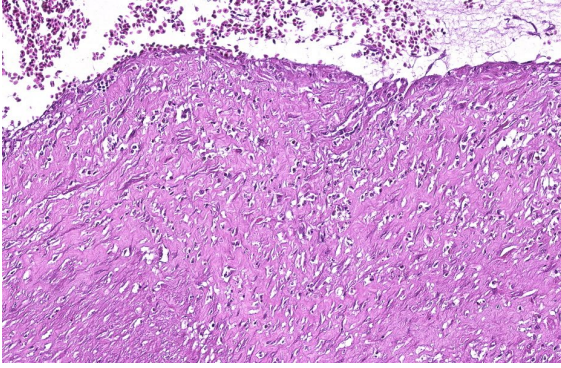
Figure 1-3. Aorta, falcon. There is loss of endothelium and marked intimal hyperplasia with fibrosis, proliferation of fibroblasts, disarray of remnant smooth muscle cells, and infiltration of macrophages. (HE, 195X)

sisting mainly of 1-day-old chicks and increased plasma cholesterol concentration and atherosclerosis when compared with a rat and mouse diet.[10]

Sudden death is the most frequent clinical manifestation of atherosclerosis in birds. It can also result in dyspnea, weakness, or neurological signs.

Grossly, early lesions are fatty streaks that progress to atheromas; there is loss of elasticity, induration, irregular thickening, and yellow discoloration of the arterial wall with narrowing of the lumen. Erosion/ulceration with thrombosis or intramural hemorrhage may occur, causing a red to brown discoloration. Atherosclerosis most commonly affects large arteries, notably the descending aorta and brachiocephalic trunks, as in the presented case.[22] Hypertrophic cardiomyopathy can also be observed in birds with atherosclerosis; however, this assessment remains subjective in raptors since there are no reference values for the dimensions of a healthy heart.[17] Some birds may show concurrent widespread xanthogranulomatosis or endogenous lipid pneumonia, suggesting a possible correlation or shared etiopathogenesis, such as dyslipidemia, for these conditions.[2,7]

Histopathologically, atherosclerotic plaques have five main components:

1. Increased cellularity of the intima with variable numbers of smooth muscle cells, macrophages, and T lymphocytes (with necrotic debris in the central core);
2. Deposition of extracellular matrix with collagen, elastin, and proteoglycans;
3. Intracellular and extracellular lipids;
4. Neovascularization at the lesion's periphery; and
5. Mineralization (in later stages).

Topographically, a luminal fibrous cap composed of smooth muscle cells and collagen overlies a layer rich in inflammatory and smooth muscle cells which borders a necrotic core containing lipids, foam cells, and cellular debris. Atheromas can be classified as vulnerable (if comprising a thin fibrous cap with large lipid core and dense inflammatory infiltrate) or stable (a thick fibrous cap or fibrous atheroma with little inflammation and lipid deposition). Possible evolution of atheromas include rupture or erosion with thrombosis of the blood vessel, intraplaque hemorrhage, atheroembolism, or aneurysm formation.[17] Several histologic classifications of avian atherosclerotic lesions have been proposed and used in pigeons, quail, chickens, and psittacine birds.[1,4,14,16,18] Some of these classification systems are based on the American Heart Association (AHA) classification of atherosclerotic lesions used in humans.[20]

Myocardial infarction and fibrosis, and medial hyperplasia of vessels of the heart, liver, lung, and kidney are reported in association with atherosclerosis in birds.[3,17] Hepatic steatosis regularly accompanies atherosclerosis,
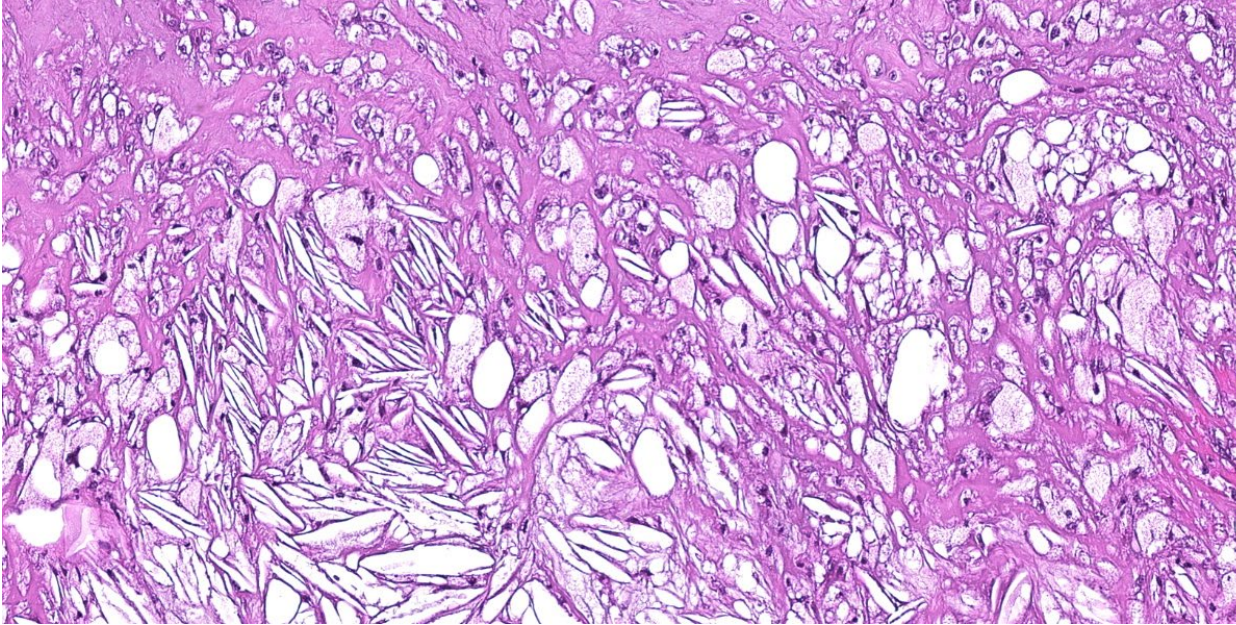
Figure 1-4. Aorta, falcon. The outer half of the tunica media is expanded by large numbers of lipophages with admixed cholesterol clefts and clear space. (HE, 266X)

suggesting a disorder of lipid metabolism.[13] In our case, the origin and significance of splenic reticuloendothelial hyperplasia and periportal hepatitis remain unclear. The presence of abundant foamy macrophages suggests a correlation with dysfunctional lipid metabolism that may have caused the atherosclerosis.

Atherogenesis has been extensively studied in humans. It is initiated by low-density lipoprotein cholesterol (LDL-C) which, when at blood concentrations in excess of physiological needs, accumulate in the intima.[11] The formation of fibrofatty atheromas (atherosclerotic plaques) includes the following sequence of events: 1) endothelial injury and dysfunction leading to increased vascular permeability, leukocyte adhesion, and thrombosis; 2) continued accumulation of lipoproteins; 3) monocyte and platelet adhesion to the endothelium and emigration of monocytes into the intima, with activation of macrophages; 4) release of factors from activated endothelial cells, macrophages (including interleukin-1, and monocyte chemoattractant protein-1), and platelets (including PDGF), inducing recruitment of smooth muscle cells; 5) smooth muscle cell proliferation, recruitment, and activation of T lymphocytes (with production of interferon gamma), and extracellular matrix deposition (notably collagen); 6) lipid accumulation within the cytoplasm of macrophages and smooth muscle cells (foam cells) and in the extracellular matrix; and 7) calcification.

Known endothelial insults in humans include hemodynamic disturbances, hypertension, hyperlipidemia, toxins (including smoke toxins), inflammation (notably from viral infection and immune reactions), and homocysteine. Atherosclerotic stenosis leads to chronic ischemia while vulnerable plaques can lead to acute and potentially fatal ischemia following rupture, thrombosis, or embolization. Compared with humans, the lymphatic system of birds is underdeveloped and birds such
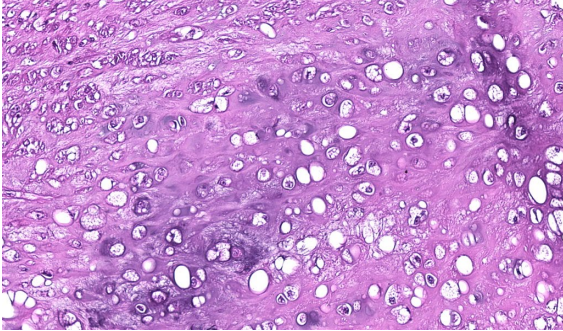
Figure 1-5. Aorta, falcon. The tunica media also contains areas of chondroid metaplasia. (HE, 368X)

as pigeons lack apolipoproteins E and B-48 and do not synthesize chylomicrons, which limits their use as models for research on the pathogenesis of human atherosclerosis.[19] Also, female birds show major changes in plasma lipoproteins during egg laying.[19]

In domestic animals, pigs, and to a lesser extent rabbits, hamsters, and chickens, are considered atherosensitive; conversely, cats, cattle, goats, and rats are atheroresistant. Although dogs are considered atheroresistant, it is not uncommon to find atherosclerosis in dogs with hypothyroidism, diabetes, or breed-related hyperlipidemia (e.g., miniature Schnauzer). Arteriolosclerosis is sporadically seen in most animal species and is considered an age-related disease. In cats with renal failure, it is a characteristic of hypertensive encephalopathy which develops because of a prolonged increase in systemic blood pressure.

Contributing Institution:
Laboratoire d'histopathologie animale
Vetagro Sup, campus vétérinaire,
http://www.vetagro-sup.fr/

JPC Diagnoses:
1. Aorta: Atherosclerosis, circumferential, diffuse, severe.
2. Epicardium: Epicarditis, fibrinous, chronic, focally extensive, moderate.

JPC Comment:
Atherosclerosis is a multifactorial disease which is well-studied in humans and often linked to defects in lipid metabolism. Though atherosclerosis is relatively rare in animals, the contributor provides an excellent overview of the clinical, demographic, gross, and histologic manifestations of atherosclerosis across a range of avian species.

In normal lipid metabolism, dietary cholesterol and triglycerides are absorbed by the gastrointestinal tract and incorporated into triglyceride-rich lipoproteins called chylomicrons.[9] These chylomicrons are subject to cleavage by endothelial enzymes and arrive at the liver as cholesterol-rich chylomicron remnants, where the cholesterol is either excreted as bile acids into the biliary tract, excreted as free cholesterol, or packaged into very low density lipoprotein (VLDL) which is then secreted into the blood.[21] VLDL is rich in triglycerides, low in cholesterol, and contains membrane apolipoproteins ApoB, ApoC, and ApoE.[9]

Once in the capillary beds of adipose tissue and muscle, VLDL undergoes lipolysis, and the resulting remnant, now with fewer triglycerides, increased cholesterol, and only containing ApoB and ApoE, is called an intermediate density particle (IDL). IDLs can be either returned to the liver to regenerate VLDLs or can undergo further lipolysis which removes most of the remaining triglycerides and ApoE, yielding a low-density lipoprotein (LDL) which is cholesterol-rich and contains only ApoB.[9]

Most LDL is taken up by the liver via the binding of ApoB to LDL receptors, and is then shuttled to lysosomes where it is metabolized to cholesterol and amino acids. Within hepatocytes, the resulting free cholesterol has an inhibitory effect on both HMG CoA re-

ductase, the rate limiting enzyme in cholesterol synthesis, and the synthesis of new LDL receptors.

Perturbation of any step of this complex pathway can result in hyperlipemia and a corresponding increased risk of atheroma formation. In humans, genetic defects in the LDL receptor are well characterized and cause familial hypercholesterolemia due to the inadequate removal of plasma LDL by the liver.[9] Similarly, mutations in the gene encoding ApoB, the ligand for LDL receptors, reduces the uptake of LDL particles by the liver, also resulting in hypercholesterolemia.

In veterinary medicine, atherosclerosis can occur naturally in many aged avian species, as detailed by the contributor, and atherosclerosis is the most common vascular lesion in the great vessels of aged psittacines and birds of prey.[8,17] Systemic hypertension is a well-known risk factor for atherosclerosis in humans and it has been suggested that the relatively higher normal blood pressures and serum cholesterol levels in birds may predispose them to atherosclerotic disease.[8]

Rabbits are also susceptible to dietary-induced hypercholesterolemia and atherosclerosis. This predisposition led to the development of Watanabe heritable hyperlipidemic rabbits, which have a genetic defect in the LDL receptor that results in aortic atherosclerosis in 100% of animals by 5 months of age.[22] The resulting disease closely mimics human atherosclerosis and Watanabe rabbits are consequently one of the main animal models used in atherosclerosis research.

Atherosclerosis has also been described in dogs, as noted by the contributor, and in pigs. Pigs do not naturally develop atherosclerosis, but can develop atherosclerotic disease similar to that seen in humans when fed high fat, high cholesterol diets.

This week's conference was moderated by MAJ Katie Scott, Chief of Necropsy at the Walter Reid Army Institute of Research (WRAIR). MAJ Scott reviewed vascular anatomy and stressed the importance of using precise anatomic terminology, particularly in conditions such as atherosclerosis where lesions are typically found in specific histologic layers (e.g., the tunica intima) due to damage to particular structural elements (e.g., the internal elastic lamina).

Several conference participants noted the fibrinous pericarditis and epicarditis present on the examined section. This finding is not typical of avian atherosclerosis and is more commonly highly pathogenic avian influenza, the latter of which was ruled out by the contributor's laboratory testing. Conference participants were suspicious that this unlucky falcon was beset by both atherosclerosis and an unknown infectious agent and chose to provide separate morphologic diagnoses for the two pathogeneses.

References:
1. Beaufrère H, Nevarez JG, Holder K, et al. Characterization and classification of psittacine atherosclerotic lesions by histopathology, digital image analysis, transmission and scanning electron microscopy. *Avian Pathol*. 2011;40(5):531–544.
2. Donovan TA, Garner MM, Phalen D, et al. Disseminated coelomic xanthogranulomatosis in eclectus parrots (*Eclectus roratus*) and budgerigars (*Melopsittacus undulatus*). *Vet Pathol*. 2022;59(1):143–151.
3. Fitzgerald BC, Beaufrère H. Cardiology. In: Speer BL, ed. *Current Therapy in Avian Medicine and Surgery*. Elsevier Health Sciences; 2016.
4. Fricke C, Schmidt V, Cramer K, Krautwald-Junghanns ME, Dorrestein GM. Characterization of atherosclerosis by

histochemical and immunohistochemical methods in African grey parrots (*Psittacus erithacus*) and Amazon parrots (*Amazona* spp.). *Avian Dis*. 2009;53: 466–472.

5. Gal A, Castillo-Alcala F. Cardiovascular system, pericardial cavity, and lymphatic vessels. In: Zachary JF, ed. *Pathologic Basis of Veterinary Disease*. 7th ed. Elsevier;2022:681-682,941-942.

6. Gisterå A, Ketelhuth DF, Malin SG, Hansson GK. Animal models of atherosclerosis: supportive notes and tricks of the trade. *Circ Res*. 2022;130(12):1869-1887.

7. Grespan A, Fiedler RT, Guedini BT, Costa LD, Raso TF. Endogenous lipid pneumonia associated with atherosclerosis in a blue-fronted Amazon parrot (*Amazona aestiva*). *J Comp Path.* 2023; 201:130-134.

8. Jones MP. Vascular diseases in birds of prey. *J Exot Pet Med*. 2013;22(4): 348–357.

9. Kumar V, Abbas AK, Aster JC. Genetic disorders. In: Kumar V, Abbas AK, Aster JC, eds. *Pathologic Basis of Disease*. 10th ed. Elsevier;2021:151-154.

10. Legler M, Kummerfeld N, Wohlsein P. Atherosclerosis in birds of prey: a case study and the influence of a one-day-old chicken diet on total plasma cholesterol concentration in different raptor and owl species. *Berl Münch Tierärztl Wochenschr*. 2017;130(7/8):353–363.

11. Libby P, Buring JE, Badimon L., et al. Atherosclerosis. *Nat Rev Dis Primers.* 2019;5(56).

12. Lujan-Vega C, Keel MK, Barker CM, Hawkins MG. Evaluation of atherosclerotic lesions and risk factors of atherosclerosis in raptors in northern California. *J Avian Med Surg*. 2021;35(3):295–304.

13. Nemeth NM, Gonzalez-Astudillo V, Oesterle PT, Howerth EW. A 5-year retrospective review of avian diseases diagnosed at the Department of Pathology, University of Georgia. *J Comp Path.* 2016;155(2-3):105–120.

14. Orita S, Masegi T, Itou K, Kawada M, Yanai T, Ueda K. Spontaneous aortic atherosclerosis in layer chickens. *J Comp Path*. 1994;110:341–347.

15. Potier, R. Lipid blood profile in captive Brahminy kite (*Haliastur indus*) as a possible indication of increased susceptibility to atherosclerosis. *J Zoo Wildl Med*. 2013;44(3):549–554.

16. Santerre RF, Wight TN, Smith SC, Brannigan D. Spontaneous atherosclerosis in pigeons. A model system for studying metabolic parameters associated with atherogenesis. *Am J Path*. 1972;1:1-22.

17. Schmidt RE, Reavill DR, Phalen DN, eds. *Pathology of pet and aviary birds*. Wiley Blackwell; 2015.

18. Shih JC, Pullman EP, Kao KJ. Genetic selection, general characterization, and histology of atherosclerosis-susceptible-and-resistant Japanese quail. *Atherosclerosis*. 1983;49(1):41–53.

19. St Clair RW. The contribution of avian models to our understanding of atherosclerosis and their promise for the future. *Lab Anim Sci*. 1998;48(6):565-568.

20. Stary HC. Natural history and histological classification of atherosclerotic lesions: an update. *Arterioscler Thromb Vasc Biol*. 200020(5):1177–1178.

21. Terio KA, McAloose D, Judy SL, eds. *Pathology of Wildlife and Zoo Animals*. Academic Press, Elsevier; 2018.

22. Tristan T. The aging raptor. *Vet Clin North Am Exot Anim Pr*. 2010;13(1):51–84.

23. Watanabe Y. Serial inbreeding of rabbits with hereditary hyperlipidemia (WHHL-rabbit). *Atherosclerosis*. 1980;36(2):261-268.

CASE II:

Signalment:
1-year-old male neutered Boxer, canine (*Canis familiaris*)

History:
The patient presented to the Oklahoma State University Veterinary Teaching Hospital with a four-week history of vomiting and weight loss.

Gross Pathology:
A segment of the proximal jejunum, approximately 34 cm long, is severely thickened to 3-4 times the normal size and is diffusely firm. The serosal surface is discolored irregularly dark red to maroon along the length of the affected segment. On cut section, the antimesenteric jejunum wall varies in thickness from 0.3-1 cm, and the wall adjacent to the mesentery is markedly thickened, ranging from 1-4 cm. The transmural thickening, especially involving the submucosa and tunica muscularis, is pale tan and densely taut (fibrous). The lumen is severely narrowed, and toward the mid-portion of the segment, is almost completely obstructed by marked thickening of the intestinal wall. The adjacent mesenteric lymph node is severely enlarged, 8x5x4 cm, and mottled yellow to tan on cut surface.

Laboratory Results:
Fungal 28S sequencing of intestine revealed 94% identity match to *Pythium insidiosum*. Lymph node sequencing was inconclusive.

Figure 2-1. Jejunum, dog. A 34 cm section of jejunum is diffusely thickened. (*Photo courtesy of:* Oklahoma State University, Department of Veterinary Pathobiology, https://vetmed.okstate.edu/veterinary-pathobiology/index.html)

Microscopic Description:
Small intestine: Three sections of jejunum are examined, each displaying mild to severe inflammation. Severely effacing multifocal and mural regions of the mucosa, submucosa, and tunica muscularis, are extensive numbers of eosinophils, accompanied by moderate to marked numbers of multinucleated giant cells (both Langhans type and foreign body type), epithelioid macrophages, and fewer numbers of lymphocytes, plasma cells, and scattered neutrophils. At the center of these inflammatory lesions, there is a moderate amount of bright, eosinophilic matrix containing karyorrhectic nuclei (necrosis), and occasionally a ghost outline of a non-staining, thin walled, 4-6 µm wide hyphae. In the most affected section, the inflammation and necrosis have distorted the villous architecture and obliterated the muscularis mucosae while dissecting through the submucosa and tunica muscularis. The submucosa is often expanded by marked amounts of fibrous connective tissue and granulation tissue. The serosa is either not affected, or markedly expanded by granulation tissue and neovascularization. Within

Figure 2-2. Jejunum, dog. An incised section of the thickened segment of jejunum. (*Photo courtesy of:* Oklahoma State University, Department of Veterinary Pathobiology, https://vetmed.okstate.edu/veterinary-pathobiology/index.html)

necrotic centers are small numbers of GMS-positive, 5-15 μm wide hyphae, with non-parallel walls, sparse to inapparent septae, and occasional branching.

Contributor's Morphologic Diagnosis:
Jejunum: Severe, segmental, chronic-active, eosinophilic and granulomatous transmural enteritis, with extensive fibrosis, granulation tissue, and small numbers of GMS-positive intralesional hyphae.

Contributor's Comment:
Gross and histologic lesions in this case are consistent with enteric pythiosis. Fungal 28S PCR sequencing revealed 94% identity match to *Pythium insidiosum* and was inconclusive for the submitted mesenteric lymph node.

Pythium insidiosum is a fungus-like, fresh water favoring, aquatic oomycete that is geographically distributed throughout the world, including southeast Asia, Australia, New Zealand, Brazil, Costa Rica, and the Caribbean.[1,5,6,8] Canine pythiosis used to be considered restricted to the states bordering the Gulf Coast in the United States; however,

there are several reports in the last two decades indicating the geography of pathogenic *Pythium insidiosum* has expanded, and now includes states within the northeast, southeast, midwest, and as far west as California.[1,4-8,10]

Recent reports have indicated that the zoospores infect mammals via ingestion, or more commonly through cutaneous lesions where the zoospores have marked chemotaxis towards injured skin, and they consequently begin to encyst on the surface of the tissue.[5,6,8] Enteric or colonic pythiosis likely occurs due to a defect within the gastrointestinal tissue allowing the zoospores to adhere and encyst.[6] *Pythium insidiosum* commonly affects horses, less often dogs and cats, and rarely affects cattle, sheep, and a few captive species including bears, camels, a tiger and a jaguar.[5-7] The remainder of this comment will focus on enteric pythiosis in canines.

The classic signalment of this disease in dogs is young, male, large breed dogs (particularly Labradors).[4,6]

Figure 2-3. Jejunum, dog. Three sections of the intestinal wall are submitted for examination and the section at bottom right is the most severely affected with marked expansion of the submucosa and muscular tunics. (HE, 5X)
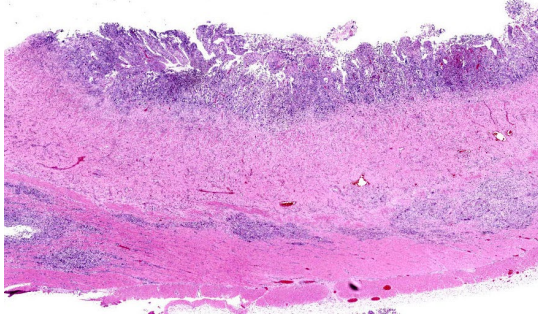
Figure 2-4. Jejunum, dog. There is transmural inflammation. The mucosal lamina propria is expanded by an inflammatory infiltrate, resulting in loss of crypts and villar blunting. The infiltrate is multifocally evident in the submucosa and muscular tunics. (HE, 15X)

The median age in most case reports is approximately 2 years old, but has been diagnosed in patients as young as 12 weeks old and as old as 6 years old.[1,4,8] Gender is evenly distributed between male and female, and large and mixed breed dogs.[1,4] Patients present with chronic, nonspecific gastrointestinal signs such as weight loss, anorexia, vomiting, and/or diarrhea.[1,4-7,10,11] Abdominal masses may be palpated during physical examination.[5,8] Clinical pathology most often reveals eosinophilia, hypoalbuminemia, and hyperglobulinemia, but may also include non-regenerative anemia and calcium irregularities (both hypocalcemia and hypercalcemia have been reported).[1,6,8]

Sites of *Pythium* infection can occur in the esophagus, stomach, small intestines, ileocecal junction, or colon, and tend to spread to adjacent mesentery and mesenteric lymph nodes.[1,4,6,8,10,11] Initial diagnostics include radiographs, ultrasound, or exploratory laparotomy, with cytology or biopsy samples submitted for ancillary testing.[6-8,11] Cytology may reveal eosinophils admixed with granulomatous to pyogranulomatous inflammation, +/- hyphae.[6] Histopathology also reveals similar findings of eosinophilic, granulomatous to pyogranulomatous inflammation with hyphal fragments located within necrotic or inflammatory centers.[4-8,10,11] The inflammation can be transmural or restricted to the submucosa and muscular layers.[6,11]

Gomori's methenamine silver (GMS) is the stain of choice for *Pythium*, as periodic acid-Schiff (PAS) poorly stains hyphae, if at all.[5,6,10] GMS characteristics include rarely septate, occasionally branching hyphae with a diameter of 2-7 μm, but can be greater than 10 μm in diameter, as was described previously in this case.[4-7,11] Care should be taken to differentiate these features from *Lagenidium* or zygomycete infections, as they have similar GMS characteristics and potentially different clinical outcomes in regards to treatment and prognosis.[6] Tests for further differentiation of these three pathogens include, but are not limited to, culture, immunohistochemistry, PCR, and ELISA.[1,5-7,10]

Prognosis is often grave depending on the duration and extent of the lesions.[1,4,6,10,11] If surgical excision is possible, it is recommended to have 3-4 cm of surgical margins.[5,6,11] Successful treatment has been reported in a few cases, and in one report of three dogs in California, treatment included the long-term use of anti-inflammatory doses of corticosteroids in conjunction with itraconazole and terbinafine.[10,11]

In conclusion, the submitted case is a classic example of *Pythium insidiosum* enteritis in a dog. The signalment and presenting complaint, in conjunction with necropsy and histologic findings, is a very common presentation of this disease, and serves as a reminder to pathologists and trainees as the distribution of this disease seems to be expanding within the United States.
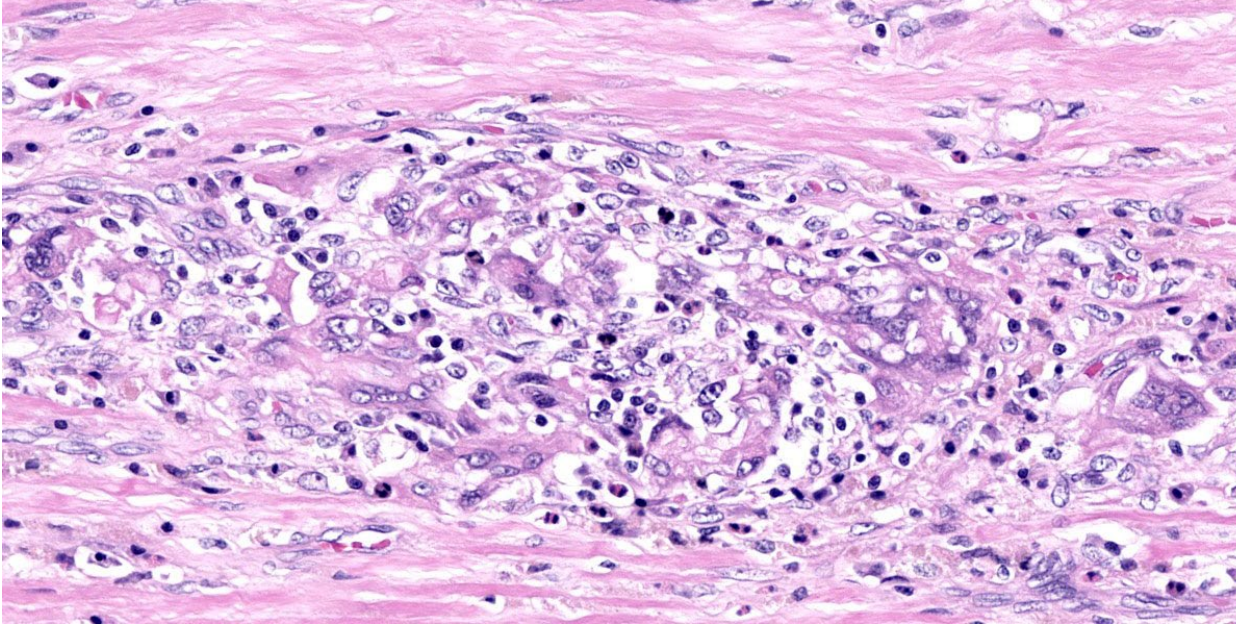
Figure 2-5. Jejunum, dog. In an inflammatory focus in the smooth muscle of the jejunal wall, there are numerous epithelioid and foreign body type macrophages. (HE, 206X)

Contributing Institution:
Oklahoma State University
Department of Veterinary Pathobiology
Stillwater, OK 740784
https://vetmed.okstate.edu/veterinary-patho-biology/index.html

JPC Diagnosis:
Small intestine: Enteritis, transmural, eosino-philic and granulomatous, moderate, with nu-merous intrahistiocytic and extracellular hy-phae.

JPC Comment:
Pythium insidiosum is famously not a fungus, but an oomycete, or "water mold." Although it forms mycelia that are rather fungus-like, its cell walls contain β-glucans and cellulose rather than chitin, its cytoplasmic membrane lacks the ergosterol characteristic of fungi, and importantly, the organism develops bi-flagellated zoospores in wet environments.[5] In some oomycetes, zoospore formation can occur in minutes on contact with water, con-sidered one of the fastest developmental pro-

cesses of any organism; however, *P. insidio-sum* is rather leisurely about the process, which takes one hour or more in this species.[5]

Once developed, these motile zoospores are chemotactically attracted to defects in mam-malian epithelium where they encyst on and adhere to injured tissues via a secreted glyco-protein. *P. insidiosum* grows optimally at mammalian body temperature, which stimu-lates the zoospores to develop hyphae that se-crete proteases to aid their extension through injured tissues, including endothelium.[5]

As hyphae penetrate tissues, they release an-tigens that are sampled by antigen presenting cells and presented to naïve T lymphocytes. The antigen presenting cells secrete IL-4, which causes the lymphocytes to assume a Th2 phenotype and secrete IL-4, IL-5, and IL-10.[5] These cytokines induce B lympho-cytes to secrete IgG, IgM, and IgE antibodies. IgE and IL-5 are chemotactic for mast cells and for the eosinophils that characterize *Pythium insidiosum* infection.[5] Summoned by cytokines, mast cells and eosinophils ar-
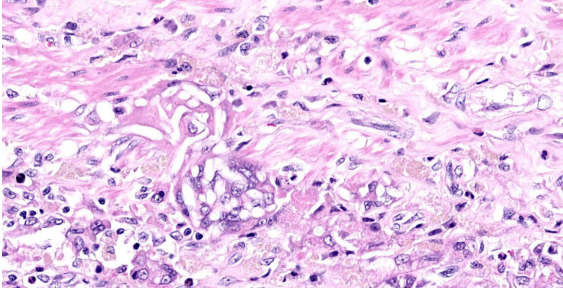
Figure 2-6. Jejunum, dog. Multinucleated foreign body giant cells contain outlines of fungal hyphae in *bas relief*. (HE, 586X)

rive at the scene and degranulate onto the hyphae, causing damage to the organism and to surrounding tissues.

The contributor provides an excellent, thorough review of canine pythiosis. Unlike canine phythiosis, equine pythiosis, also known by the memorable name "swamp cancer," most commonly affects the skin; the intestinal disease seen in dogs is rarely reported in horses.[5] Equine cutaneous lesions occur in skin in contact with water, such as the lower limbs and ventral abdomen, and grossly appear as large, round, granulomatous, ulcerated tissue. On histology, these lesions are granulomatous and characterized by eosinophils and poorly-staining *P. insidiosum* hyphae. The horse uniquely develops multilobulated, irregular cores of necrotic yellow material known as "kunkers," which are formed from degranulated eosinophils and hyphae.[5]

Sheep can develop cutaneous or digestive pythiosis that is substantially similar to the disease in horses and dogs; however, sheep also have their own flavor of pythiosis called ovine rhinofacial pythiosis, or "bull nose."[3] This disease, reported exclusively in Brazil, is an important cause of death and economic loss and is characterized clinically by marked enlargement and deformity of the nasal region, difficulty breathing, and epistaxis.[3] The gross lesion typically extends from the mucocutaneous junction of the nares to the middle nasal cavity and can involve adjacent facial

structures, such as the nasal septum and hard palate.[3]

Pythiosis occurs only sporadically in other species. In cats, the disease typically affects the skin and subcutis, but without the ulceration that is common in other species.[3] Cattle in rainy, subtropical climates are sporadically affected, typically on the limbs, by fistulated, ulcerated masses composed of eosinophilic granulomas centered on hyphae.[5] There have been only two reports of pythiosis in birds: ulcerative eosinophilic granulomas in the wings, head, neck, and limbs of a white-faced ibis;[9] and a transmural, necrotic, obstructive esophageal mass filled with heterophils, eosinophils, and hyphae in the esophagus of a red-necked ostrich.[2]

Conference discussion focused on the unique features of this organism, including its dimorphic life cycle, unique cell wall composition, and the inability to differentiate *Pythium* spp. from *Lagenidium* spp. and from the zygomycetes (*Conidiobolus* spp. and *Basidiobolus* spp.) without molecular methods such as PCR.
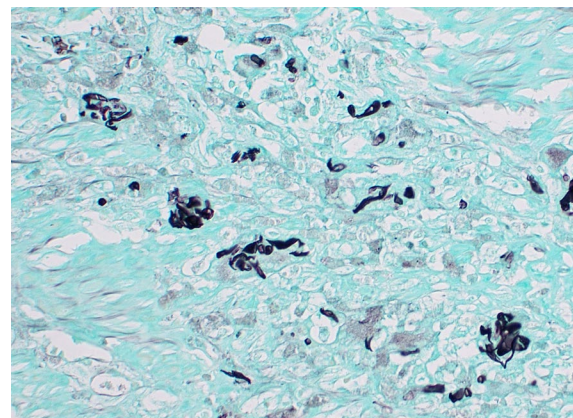

Figure 2-7. Jejunum, dog. A silver stain demonstrates the presence of fungal hyphae within foci of inflammation. (GMS, 400X)

References:

1. Berryessa, NA, Marks SL, Pesavento PA, et al. Gastrointestinal pythiosis in 10 dogs from California. *J Vet Intern Med*. 2008; 22:1065-1069.
2. de Souto EPF, Kommers GD, Souza AP, et al. A retrospective study of pythiosis in domestic animals in northeast Brazil. *J Comp Pathol*. 2022;195:34-50.
3. do Carmo PMS, Uzal FA, Riet-Correa F. Diseases caused by *Pythium insidiosum* in sheep and goats: a review. *J Vet Diagn Invest*. 2021;33(1):20-24.
4. Fischer, JR, Pace LW, Turk JR, Kreeger JM, Miller MA, Gosser HS. Gastrointestinal pythiosis in Missouri dogs: eleven cases. *J Vet Diagn Invest.* 1994; 6:380-382.
5. Gaastra W, Lipman LJA, De Cock AWAM, et al. Pythium insidiosum: An overview. *Veterinary Microbiology.* 2010;146:1-16.
6. Grooters, A. Pythiosis, lagenidiosis, and zygomycosis in small animals. *Vet Clin Small Anim.* 2003; 33:695-720.
7. Kepler D, Cole R, Lee-Fowler T, Koehler J, Shrader S, Newton J. Pulmonary pythiosis in a canine patient. *Vet Radiol Ultrasound*. 2019; 60:E20-E23.
8. Liljebjelke KA, Abramson C, Brockus C, Greene CE. Duodenal obstruction caused by infection with Pythium insidiosum in a 12-week-old puppy. *JAVMA*. 2002; 220(8):1188-1191.
9. Pesavento PA, Barr B, Riggs SM, Eigenheer AL, Pamma R, Walker RL. Cutaneous pythiosis in a nestling white faced ibis. *Vet Pathol*. 2008;45:538-541.
10. Reagan KL, Marks SL, Pesavento PA, Maggiore AD, Zhu BY, Grooters AM. Successful management of 3 dogs with colonic pythiosis using itraconazole, terbinafine, and prednisone. *J Vet Intern Med.* 2019; 33:1434-1439.
11. Schmidt CW, Stratton-Phelps M, Torres BT, et al. Treatment of intestinal pythiosis in a dog with a combination of marginal excision, chemotherapy, and immunotherapy. *JAVMA*. 2012; 241 (3):358-363.

CASE III:

Signalment:
27-week-old female laying hen, avian (*Gallus gallus domesticus*)

History:
A laying hen farm with 6 houses and a total of 180,000 animals reared in enriched cages showed an episode of severe respiratory clinical signs in one of the houses with 24-week-old laying hens. The process was diagnosed as an outbreak of infectious laryngotracheitis (ILT) based on compatible severe respiratory signs and consistent gross lesions and was further confirmed by PCR. One month later, the birds continued displaying severe respiratory signs and similar gross lesions at postmortem examinations, but with fewer fibrinonecrotic intratracheal casts and proliferative mucosal lesions. Information regarding productive parameters or total flock mortality was not revealed by the producer. Four chickens were submitted for gross postmortem examination, and formalin-fixed samples of the tracheas were submitted for further histopathological evaluation in the diagnostic facilities. The batch had been vaccinated at 8 weeks against *Gallid herpesvirus 1* (GaHV-1) with an eye drop attenuated live vaccine and against fowlpox virus (FWPV) with an attenuated live vaccine by wing web vaccination. Vaccination against other common pathogens was performed following routine vaccination protocol.

Figure 3-1. Trachea, chicken. The tracheal epithelium is diffusely hyperplastic and there is a luminal plug of necrotic epithelium and inflammatory cells. (HE, 5X)

Gross Pathology:
All tracheas showed similar changes. The tracheal wall was moderately to markedly thickened, conferring a pipe-stem appearance, which greatly narrowed the tracheal lumen. Tracheal lumina were variably occluded by white dense casts.

Laboratory Results:
PCR assays for *Gallid herpesvirus 1* (GaHV-1) and fowlpox virus (FWPV) performed on tracheal samples were positive for both pathogens.

Microscopic Description:
The tracheal lumen is markedly narrowed due to a massive circumferential thickening of the tracheal mucosa, consisting of hyperplastic and hypertrophic epithelial cells. These epithelial cells frequently display cytoplasmic tumefaction and rarefaction (ballooning degeneration). A single 15-50 µm round or ring-shaped eosinophilic inclusion is observed in the cytoplasm of many of the epithelial cells (Bollinger body). In the tracheal lumen large amounts of necrotic debris, degenerated heterophils, abundant bacterial colonies, eosinophilic fibrillar material (fibrin) and mucus are also observed. There are several syncytial cells containing 5-15 nuclei with 3-6 µm eosinophilic intranuclear inclusion bodies that marginate the chromatin and are surrounded by a clear halo. The lamina propria is further expanded by abundant lymphoplasmacytic and, to a lesser extent, heterophilic infiltration.

Contributor's Morphologic Diagnoses:
1. Trachea: Diffuse, circumferential, subacute, severe, hyperplastic, and necrotizing tracheitis with intralesional Bollinger bodies.
2. Trachea: Diffuse, circumferential, subacute, severe, fibrinonecrotizing tracheitis with intralesional syncytial cells and intranuclear inclusion bodies.

Contributor's Comment:
Poultry viral infections are common causes of disease and economic loss and are thus major concerns in poultry production. Infectious laryngotracheitis (ILT) is a respiratory disease of chickens, pheasants, and peafowl which is caused by *Gallid herpesvirus 1* (GaHV-1), an alphaherpesvirus.[8] ILT can cause large economic losses in high density poultry-producing regions; consequently, many efforts are focused on diagnosing and controlling ILT through vaccination, mainly in the form of live attenuated vaccines.[2] These vaccines generally prevent and reduce the severity of the disease and associated mortality, although birds may become latent carriers and shedders of vaccinal viruses. Occasionally, transmission of these vaccinal viruses can occur, enabling viruses to regain virulence and produce mortality, particularly when vaccines are administered in the drinking water or in spray or when Chicken Embryo Origin (CEO) vaccines (as in our case) are used.[6]
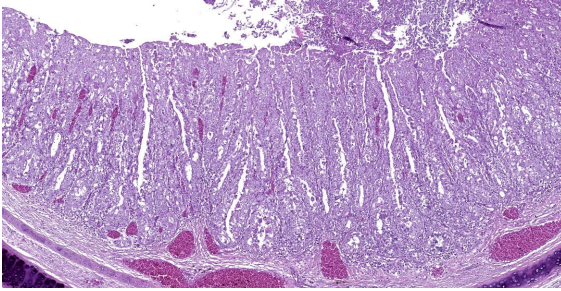
Figure 3-2. Trachea, chicken. The tracheal epithelium thrown into thick villar folds. (HE, 79X)

Virulence is variable across GaHV-1 strains, which results in ILT having variable degrees of severity. In all cases, virus replicates in epithelial cells across the respiratory tract and conjunctiva, causing severe epithelial damage and accounting for the clinical signs which usually include nasal discharge, conjunctivitis, moist rales, dyspnea, and expectoration of blood-stained mucus. In severe cases, mucoid casts in the trachea obstruct the airways and lead to asphyxiation.[11]

All these signs correlate with the presence of gross and microscopic findings, which include mucoid to necrotizing tracheitis, frothy ocular secretions, and swelling of infraorbital sinuses caused by epithelial degeneration and necrosis of the previously mentioned tissues. Microscopically, this epithelial damage is often accompanied by lymphocytic and heterophilic inflammation and by syncytial cells with nuclear inclusions, characterized by strong eosinophilic staining surrounded by clear halos. These nuclear inclusions are commonly used as a powerful diagnostic technique as they are pathognomonic for ILT, although they are only present between days 2 and 5 post infection.[11] Birds that survive this acute phase display hyperplastic changes of the epithelium lining the respiratory tract after the first wave of necrosis with absence of syncytial cells and inclusions, which

limits histological diagnosis.[1] In the absence of nuclear inclusions, molecular techniques are needed for definitive diagnosis.

Other significant avian pathogens include viruses of the *Poxviridae* family, which includes the genus *Avipox*. Fowlpox virus (FWPV) affects commercial poultry with variable disease manifestations, including cutaneous or diphteric/pharyngeal forms. In the poultry industry, this disease, commonly referred to as fowlpox, is controlled through live modified virus vaccines, which prevent disease manifestations and further production implications.[3] Despite vaccinal efficacy, numerous outbreaks in vaccinated flocks have been reported. Emergence of variant strains of FWPV and enhanced virulence due to the integration of avian reticuloendotheliosis virus (REV) into their genomes are believed to be the main causes of outbreaks in vaccinated animals.[9] Viral genome sequencing was not performed in our case in order to rule out these possibilities. Furthermore, technical vaccine failure cannot be fully ruled out.

Viral replication of FWPV occurs in epithelial cells of the skin and upper alimentary and respiratory tracts, which provoke hyperplastic and proliferative lesions characteristic of poxvirus infections. These lesions are represented grossly by cankers, elevated nodules or patches, and diphteric yellowish lesions in the mucous membranes of the mouth, oesophagus or trachea. These lesions account for the severe respiratory signs commonly exhibited by affected birds. Histologically, affected epithelium is hyperplastic and hypertrophic and undergoes necrosis in the apical region. Infected epithelial cells frequently display large intracytoplasmic inclusion bodies, which are called Bollinger bodies.[11]
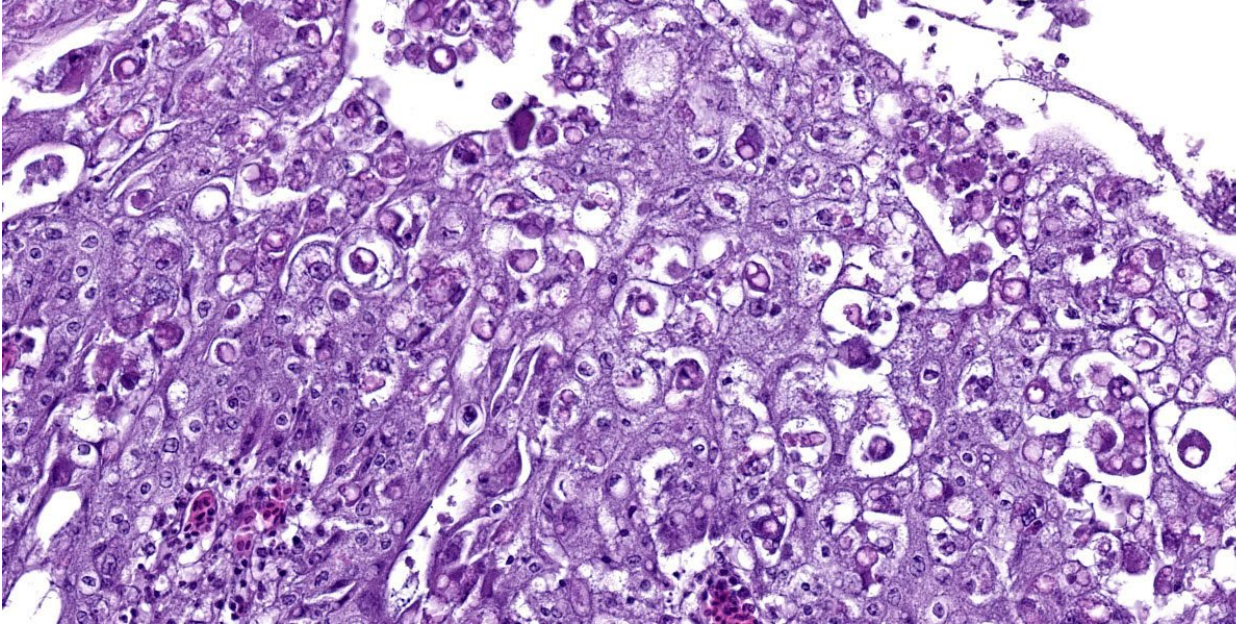
Figure 3-3. Trachea, chicken. The tracheal epithelium exhibits ballooning degeneration with large intracytoplasmic poxviral inclusions ("Bollinger bodies"). (HE, 200X)

Both GaHV-1 and FWPV can result in severe respiratory signs, and significant overlap exists in their clinical signs and gross lesions. To reach definitive diagnosis, samples are usually sent to diagnostic facilities and confirmation is based on histopathological evaluation or molecular diagnostics. Observation of typical viral inclusions of either of the infections is a usual path to definitive diagnosis. Nevertheless, simultaneous dual infections have been described in commercial chickens, and although not common due to generally effective vaccination, the characteristic histological lesions and inclusion bodies of both viruses can appear in the same tracheal section, as in this case.[5,10]

Contributing Institution:
Veterinary Pathology Department
Autonomous University of Barcelona
Barcelona, Spain.
https://www.uab.cat/

JPC Diagnoses:
1. Trachea: Tracheitis, proliferative and necrotizing, circumferential, severe, with ballooning degeneration, and intracytoplasmic viral inclusions.
2. Trachea: Tracheitis, necrotizing, circumferential, with few viral syncytia and intranuclear inclusions.

JPC Comment:
Infectious laryngotracheitis (ILT) has a narrow natural host range when compared with other alphaherpesviruses, and is primarily a disease of chickens. The disease is highly contagious and infected birds shed the virus in their respiratory secretions for 10 days post-infection.[7] GaHV-1 can infect the host via respiratory, ocular, or oral routes, and can be spread by direct transmission from an infected bird or a latent carrier, or through fomites such as litter, feed bags, feathers, dust, footwear, and clothing.[7]

Once inside the animal, replication in the conjunctival, sinus, laryngeal, and tracheal epithelium leads to inflammation, serous or mucoid nasal and ocular discharge, and respiratory distress.[4] The key histologic features
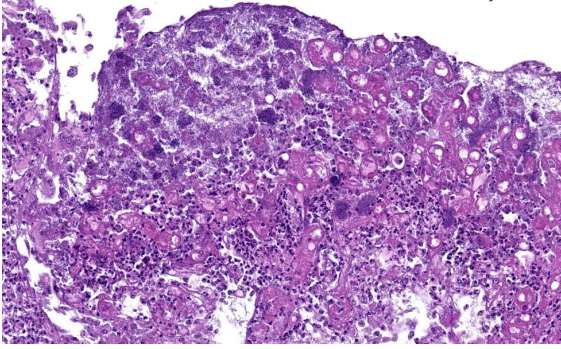
16

Figure 3-4. Trachea, chicken. The luminal plug is composed of sloughed pox-virus-laden epithelium, infiltrating necrotic and viable neutrophils, abundant cellular debris, and numerous bacterial colonies. (HE, 200X)

used to diagnose ILT are syncytial cells with intranuclear inclusion bodies, most frequently present in the trachea, nasal turbinates and sinuses, conjunctiva, larynx, and primary bronchi.[4] With disease progression, the laryngeal and proximal tracheal epithelium sloughs into the lumen, forming an exudate that accumulates in the syrinx, and this necrosis and sloughing of the superficial epithelium likely accounts for the loss of identifiable syncytial cells by 5 days post-infection.[4]

The virulence of ILT varies with the infecting strain and is exacerbated by concurrent infection with other respiratory pathogens such as *Mycoplasma gallisepticum, Mycoplasma synoviae*, infectious coryza, and reticuloendotheliosis virus, as well as immunosuppression, including immunosuppression secondary to Marek's disease.[7] If the animal survives, ILT virus may flock to the trigeminal ganglion and, like any good herpesvirus, may establish a life-long latent infection that can be reactivated during periods of stress.

The clinical signs of ILT are similar to those of other viral respiratory diseases of chickens, including Newcastle Disease, Fowl Pox, Infectious Bronchitis, and Avian Influenza.

These diseases can typically be differentiation with histology. In Newcastle disease, surface epithelium is usually still intact, in contrast to the necrosis and sloughing seen with ILT, and multiple organ systems are affected. Fowl pox, as seen in this case, is characterized by large eosinophilic *cytoplasmic* viral inclusions (Bollinger bodies) in contrast to the much smaller, intranuclear viral inclusions of early ILT infection; affected epithelium is proliferative rather than necrotic; and syncytial cells are absent. Finally, infectious bronchitis and avian influenza typically affect a wider range of tissues, most notably the lower respiratory tract.

In conference, the moderator led a discussion of the biology of the two viruses implicated in this case and discussed ways to simplify infectious disease pathology by grouping viruses and bacteria into "boxes" with similar behaviors. The "Pox box" was opened, and participants were treated to a review of the some of the more singular poxviruses, including ectromelia, rabbit (Shope) fibroma virus, and myxoma virus.

As the contributor notes, the two concurrent diseases in this case have overlapping histologic features and considerable conference discussion centered on whether it was possible to attribute particular histologic lesions with a specific etiology.
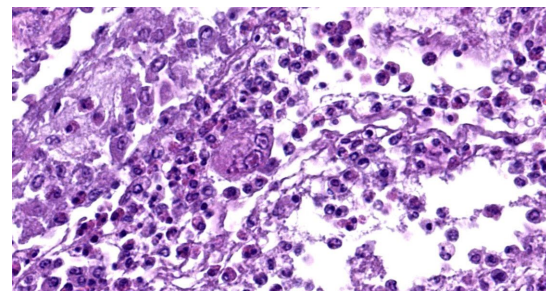

Figure 3-5. Trachea, chicken. Rare multinucleated epithelial cells within the luminal plug contain herpeviral intranuclear inclusions. (HE, 892X)

In the end, participants settled on a pair of morphologic diagnoses that, in their redundancy, acknowledge these overlapping clinical and histologic features.

References:
1. Abdul-Aziz T, Fletcher OJ, Barnes HJ. *Avian histopathology*. 4th ed. American Association of Avian Pathologists; 2016.
2. Bagust TJ, Jones RC, Guy JS Avian infectious laryngotracheitis. *Rev. Sci. Tech.* 2000;19(2):483–492.
3. Bolte AL, Meurer J, Kaleta EF. Avian host spectrum of avipoxviruses. *Avian Pathol.* 1999;28(5):415-432.
4. Carnaccini S, Palmieri C, Stoute S, Crispo M, Shivaprasad HL. Infectious laryngotracheitis of chickens: pathologic and immunohistochemistry findings. *Vet Pathol*. 2022;59(1):112-119.
5. Davidson I, Raibstein I, Altory A. Differential diagnosis of fowlpox and infectious laryngotracheitis viruses in chicken diphtheritic manifestations by mono and duplex real-time polymerase chain reaction. 2014; *Avian Pathol.* 2015;44(1):1-4.
6. García, M. Current and future vaccines and vaccination strategies against infectious laryngotracheitis (ILT) respiratory disease of poultry. *Vet. Microbiol.* 2017;206:157–162.
7. Gowthaman V, Kumar S, Koul M, et al. Infectious laryngotracheitis: etiology, epidemiology, pathobiology, and advances in diagnosis and control: a comprehensive review. *Vet Q.* 2020;40(1):140-161.
8. Menendez KR, García M, Spatz S, Tablante NL. Molecular epidemiology of infectious laryngotracheitis: a review. *Avian Pathol*. 2014;43(2):108-17.
9. Singh P, Kim TJ, Tripathy DN. Reemerging fowlpox: evaluation of isolates from vaccinated flocks. *Avian Pathol.* 2000;29(5):449-455.
10. Song HS, Kim HS, Kim SH, Kwon YK, Kim HR. Research Note: Simultaneous detection of infectious laryngotracheitis virus, fowlpox virus, and reticuloendotheliosis virus in chicken specimens. *Poult. Sci.* 2021;100(4):100986.
11. Swayne DE, ed. *Diseases of poultry*. 14th ed. Wiley; 2019.

CASE IV:

Signalment:
1-year-old male castrated Boxer, canine (*Canis familiaris*)

History:
The patient presented to the Matthew J. Ryan Veterinary Hospital of the University of Pennsylvania (MJR-VHUP) emergency service with a history of two swellings/masses on the left ventral jaw and adjacent to the left nostril as well as acute vomiting, weight loss, hyporexia, and lethargy. The masses were originally noted by the primary veterinarian who started systemic antibiotics. Over the 14-day course of antibiotics, the masses reduced in size, but subsequently rapidly grew upon completion of the course of antibiotic therapy. Due to the lack of resolution, the primary veterinarian performed a sedated oral exam, skull radiographs, and bloodwork approximately 3 weeks after the patient's initial presentation. The radiographs demonstrated regional soft tissue swelling but no obvious intraoral component. The complete blood count showed a neutrophilic leukocytosis. The patient became progressively lethargic and hyporexic over the following 24 hours and was presented to the emergency service at MJR-VHUP the next day.

On clinical examination at MJR-VHUP, there was an approximately 10 cm diameter, firm, moveable mass on the left ventrocaudal

Figure 4-1. Skeletal muscle, heart, lung, dog. A metastatic neoplasm is present in these three submitted tissues. (HE. 5X)

face at the level of the mandible, which extended to the level of the left maxilla. The mass caused partial occlusion of the left naris and lateral deviation of the nose. The patient was hospitalized and transferred to the Internal Medicine service. Over the course of the patient's 3-day hospitalization, an abdominal ultrasound and thoracic radiographs were performed, which revealed multiple soft tissue nodules throughout the thoracic and abdominal cavity. Subsequent physical exams revealed additional masses on the left shoulder and within the left and right epaxial muscles. Fine needle aspirates of the left facial/submandibular mass revealed a malignant neoplasm. Due to the rapid, aggressive progression of disease and poor prognosis, euthanasia was performed and a full postmortem examination was completed.

Gross Pathology:
Extending from the rostral muzzle just left of midline to the ventral submandibular region was a 16 x 8 x 6 cm multilobulated, variably firm to hard, white and tan mass that infiltrated through the right nasal bone and rostral hard palate, into the nasal cavity, and expanded the nasal turbinates and displaced the maxillary incisors. On cut surface within the individual neoplastic lobules, the center of the tissue was dark red to brown and variably soft to gelatinous. Similar multilobulated and

sometimes cavitated nodules, ranging from 1 cm diameter to 7 x 4 x 2 cm, infiltrated the skeletal muscle of the caudal aspect of the left shoulder, left craniolateral abdominal body wall, left superficial inguinal subcutis, left midabdominal epaxial, and right lumbar epaxial muscles.

Within the thoracic cavity, innumerable nodules expanded the mediastinum, pericardium, pleural surfaces of the thoracic walls, myocardium, and pulmonary parenchyma. Within the abdominal cavity, the omentum, left lobe of the pancreas, and left adrenal gland were expanded by similar nodules. The cavitated nodules often contained a small to moderate amount of dark brown watery to yellow-brown thick opaque fluid. The thoracic cavity contained approximately 1150 mL of watery, light red, opaque fluid.

The left retropharyngeal, left axillary, tracheobronchial, sternal, and mediastinal lymph nodes were enlarged (measuring up to 6 x 1 x 2 cm), had loss of corticomedullary distinction, and were effaced by similar tissue as described above.

Laboratory Results:
Tissue culture from the mass yielded no growth on aerobic or anaerobic cultures.

Antemortem cytology of the left mandibular mass showed neoplastic cells amid a light pink, stippled proteinaceous background. Neoplastic cells were pleomorphic, mainly round when individualized, occasionally spindled, and slightly polygonal when seen in clusters. Nuclei were round to irregularly shaped, with reticular chromatin and occasionally visible light blue irregular nucleoli. There was a scant to moderate amount of deep blue cytoplasm with frequent blebbing, paranuclear clearing, and several distinct vacuoles, rarely containing 1-2 small dark blue/green granules. Mitotic figures were
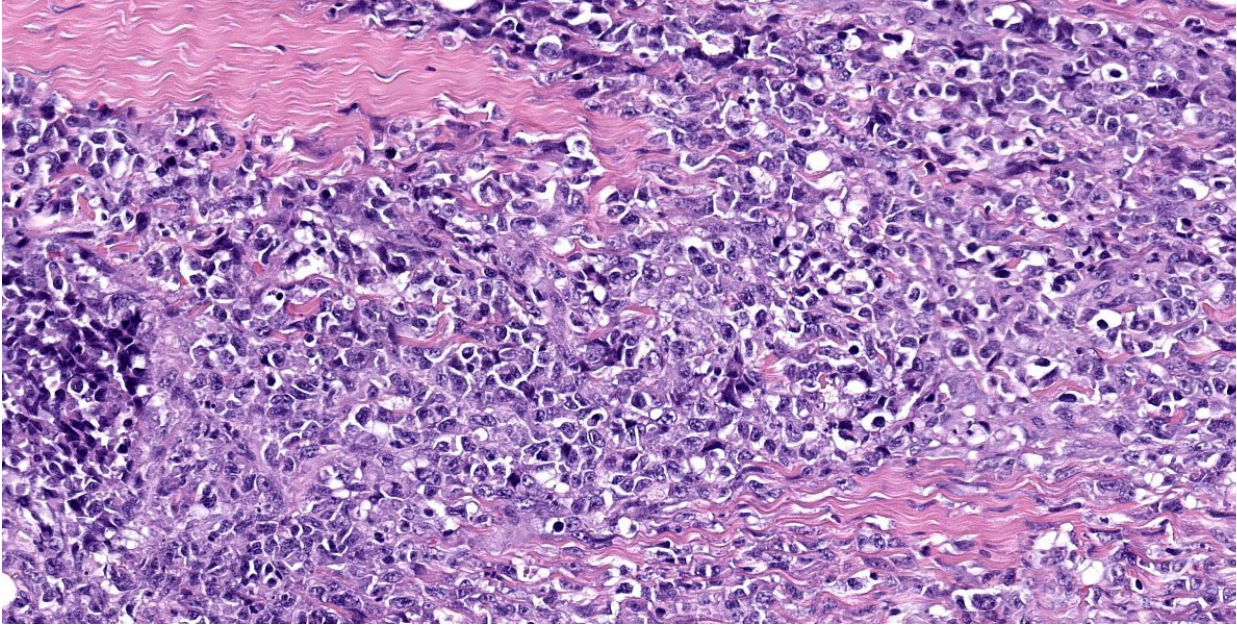
Figure 4-2. Skeletal muscle, dog. The muscle is effaced by sheets of pleomorphic cells. (HE, 319X)

moderately frequent and contained atypical forms.

The cytology sample was diagnosed as a malignant neoplasm, with the primary differential diagnoses including a poorly melanotic/amelanotic melanoma, epithelioid hemangiosarcoma, rhabdomyosarcoma, anaplastic carcinoma, or other embryonal tumor.

Microscopic Description:
Skeletal muscle from the face: One section of skeletal muscle from the face is examined. The tissue architecture is infiltrated to completely effaced by an unencapsulated, densely cellular neoplasm, composed of round to polygonal to spindle-shaped cells arranged in sheets, bundles, streams, and packets separated by a fine fibrovascular stroma. Neoplastic cells have variably distinct cell borders with a scant to moderate amount of eosinophilic to amphophilic cytoplasm and round to ovoid nuclei with open chromatin and a single variably prominent nucleolus. Anisocytosis and anisokaryosis are moderate to marked and there are up to 23 mitotic figures in a single 40x high power field (0.237

mm2). There are multifocal regions of necrosis throughout the neoplastic parenchyma. The skeletal muscle fibers incorporated amongst neoplastic cells exhibit varying degrees of degeneration and necrosis, including hypereosinophilic and swollen to fragmented, amphophilic and granular sarcoplasm.

Heart: One full thickness section of the right ventricular free wall is examined. Within the myocardium and extending through the epicardial surface, there is an infiltrative unencapsulated densely cellular neoplasm comprised of spindle-shaped to polygonal cells arranged in haphazard streams and packets with a scant fibrous stroma. Neoplastic cells are similar to those described in the facial skeletal muscle with large regions of coagulative necrosis scattered throughout the parenchyma. The incorporated myocardial muscle fibers are surrounded by neoplastic cells and demonstrate shrunken angular sarcoplasm (atrophy).

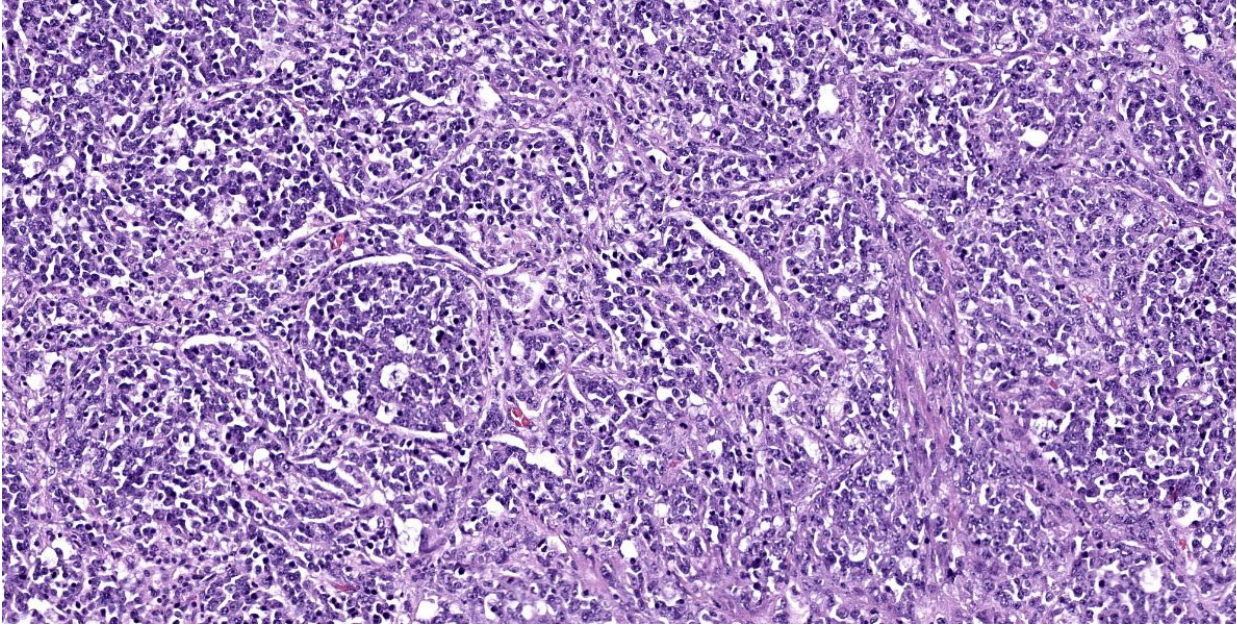Lung: One section of lung is examined. Within the pulmonary parenchyma, occasionally surrounding large blood vessels,

Figure 4-3. Lung, dog. Neoplastic cells expand alveolar septa and fill alveoli. (HE, 87)

there are multiple variably well-defined to infiltrative, unencapsulated, densely cellular foci of similar round to polygonal neoplastic cells arranged in sheets and packets amongst a fine stroma forming thin fibrous septa. Neoplastic cells infiltrate along the pleural surface and are present within small pulmonary vessels and alveolar capillaries. Adjacent to the neoplastic nodules, there is minimal to mild pulmonary edema with increased numbers of foamy macrophages within the alveolar lumen.

Immunohistochemical staining with PNL2, desmin, CD3, and CD79b were performed on sections of the neoplasm in the skeletal muscle of the face. Neoplastic cells were diffusely negative for PNL2, CD3, and CD79b. Greater than 90% of the neoplastic cells exhibited strong, diffuse, cytoplasmic immunoreactivity with desmin.

Tissues pertinent to the clinical presentation but not included in the submission include the rostral maxillary bone, nasal cavity, and liver. The cortical bone of the rostral maxilla and hard palate was disrupted and effaced by ne-

oplastic cells, which extended into the submucosa of the overlying gingiva and rostral nares. The centrilobular sinusoids within the liver were mildly dilated and filled with blood, interpreted as mild acute passive congestion.

Contributor's Morphologic Diagnoses:
1. Skeletal muscle: Rhadomyosarcoma.
2. Heart and Lung: Metastatic rhadomyosarcoma.

Contributor's Comment:
Based on the clinical history, patient signalment, and cellular morphology on histopathology, differentials for the neoplasm included an amelanotic malignant melanoma, lymphoma, or embryonal tumor, such as a rhabdomyosarcoma of juvenile dogs. The immunohistochemical staining profile is compatible with a rhabdomyosarcoma. The maxillofacial region is favored as the site of origin for this neoplasm, given the clinical history and degree of local invasion; however, with the extensive multi-organ involvement and overall poor cellular differentiation, a different primary location is not entirely ruled out.
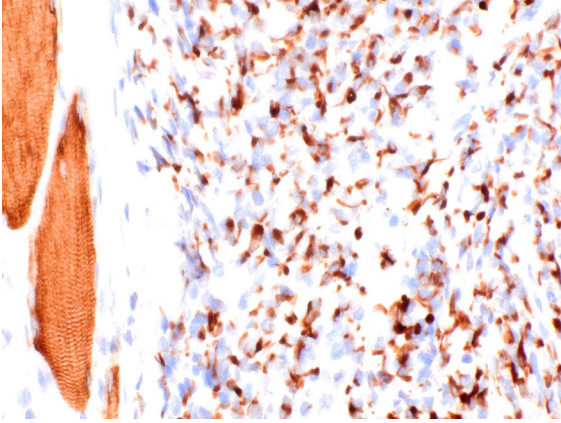
**Figure 4-4. Skeletal muscle, dog. Neoplastic cells demonstrate strong cytoplasmic immunoreactivity to desmin. (*Photo courtesy of: University of Pennsylvania School of Veterinary Medicine, Department of Pathobiology, https://www.vet.upenn.edu/veterinary-hospitals/ryan-veterinary-hospital/services/diagnostic-laboratories). (anti-desmin, 400X)*

Rhabdomyosarcoma (RMS) is a malignant neoplasm of skeletal muscle derived from pluripotent stem cells or mesenchymal progenitor cells capable of myogenic differentiation.[2] This neoplasm is relatively rare in veterinary species and the current literature suggests this neoplasm more commonly arises in dogs younger than 2 years of age.[2,3] In the human medical literature, RMS is considered a common head and neck tumor of children.[7] Immunohistochemistry is commonly utilized to differentiate RMS from other neoplasms because of the variable microscopic appearance, primary locations, and frequent lack of well-differentiated skeletal muscle within RMS. Due to the inconsistent and variable staining properties, as well as lack of specificity of more commonly available skeletal muscle markers (i.e. desmin), a recent publication suggests the use of immunohistochemical markers MyoD1 and myogenin in conjunction with desmin, to improve the accuracy of diagnosing these challenging tumors.[12]

Following the histologic classification criteria outlined in the Caserto 2013 review, the RMS in this case had features consistent with a solid alveolar subtype, characterized by the majority of the neoplastic foci arranged in sheets of round cells closely packed together and divided by thin fibrous septa, reminiscent of a "neuroendocrine pattern." Within the current veterinary literature, this subtype is less frequently diagnosed; however, the true incidence of the different subtypes is unclear given the diagnostic challenge and IHC often needed to make a definitive diagnosis. There is little supporting outcome data in veterinary literature to evaluate prognosis between different subtypes; however, alveolar RMS are considered more locally aggressive with a higher metastatic rate in human patients.[2,10] Case reports of this subtype of canine RMS in the veterinary literature frequently note significant local invasion into the maxilla and an overall, poor clinical progression of disease, similar to what was seen in this case.[4,5,7-9] Other primary locations reported in the human and veterinary literature include the urogenital tract, retroperitoneum, tongue, oral cavity, larynx, skin, heart, and peripheral appendicular and axial skeletal muscle.

Perhaps due to the aggressive disease progression, poor prognosis, and euthanasia at time of initial diagnosis, metastatic rate and sequelae are relatively less frequently discussed in regards to RMS of juvenile dogs; however, a striking feature of this case is the staggering metastatic disease throughout peripheral lymph nodes, skeletal muscle, and thoracic and abdominal cavities. The aggressive nature and pathogenesis of metastasis in human alveolar and embryonal RMS have been attributed to several mutations in transcription factors. A mutation as a result of translocation and fusion of the PAX-FKHR genes has been shown to result in uncontrolled cell growth, progression through the
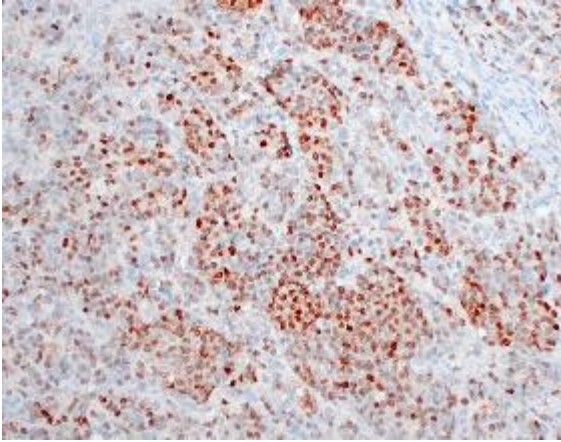
Figure 4-5. Skeletal muscle, dog. Neoplastic cells demonstrate strong nuclear immunoreactivity to myoblast determination protein. (anti-myoD1, 400X)

cell cycle, and loss of tumor suppressor function, and is considered a significant factor in the aggressive phenotype seen in alveolar RMS.[2] The transcription factors LMO4 and FOXF1 are involved in tumor migration and are shown to be overexpressed in RMS with distant metastasis.[1] Snail1, a transcription factor associated with epithelial-mesenchymal transition, is shown to be highly expressed in alveolar RMS. It is presumed that this contributes to the downregulation of E-cadherin and increased expression of matrix metalloproteinases (MM2 and MM9), further promoting tumor invasion and metastasis.[1] The IL4 receptor signaling pathway in RMS has also been shown to recruit myoblasts to form mature myotubes, stimulate cell proliferation through the JAK/STAT signaling pathway, and may be involved with lymph node and pulmonary metastasis via CD4+ T cell/TH2 cell activation of tumor-associated macrophages.[6] While these specific factors have not been studied in veterinary species, it is possible that a similar tumor pathogenesis contributes to the aggressive behavior of this neoplasm in dogs.

In this case, the patient's clinical decline is attributed to the extensive metastatic disease leading to multi-organ dysfunction. Given the degree of neoplastic infiltrate within the myocardium, it is presumed there was some degree of cardiac dysfunction resulting in early congestive heart failure, demonstrated by the pathologic changes of acute passive congestion in the liver and significant pleural effusion. Furthermore, the local neoplastic invasion into the maxilla combined with extensive multi-organ involvement likely contributed to the patient's hyporexia and ultimately the progression of clinical disease.

Contributing Institution:
University of Pennsylvania
School of Veterinary Medicine
Department of Pathobiology
https://www.vet.upenn.edu/veterinary-hospi-tals/ryan-veterinary-hospital/services/diag-nostic-laboratories

JPC Diagnosis:
Skeletal muscle, heart, lung: Rhabdomyosarcoma, alveolar type.

JPC Comment:
As the contributor notes, rhabdomyosarcoma (RMS) presents a diagnostic challenge due to its variable histomorphology and lack of evident skeletal muscle differentiation on light microscopic evaluation. Skeletal muscle begins its developmental journey as embryonic mesoderm that differentiates into myogenic progenitor cells under the control of transcription factors such as PAX3 and PAX7.[2] These myogenic progenitor cells proliferate and form immature myoblasts under the direction of myoblast determination protein 1 (MyoD1), a transcription factor that acts at hundreds of gene promoters to drive myoblast proliferation.[2] Via an unknown mechanism, myoblasts fuse and elongate and their nuclei line up in rows, forming myotubes with multiple nuclei and shared cytoplasm. Myogenin, a transcription factor in the same family as MyoD1, then directs the myotubes

to begin producing actin and myosin-containing sarcomeres that are characteristic of skeletal muscle.[2] Myogenin causes cell cycle arrest, leading to terminally differentiated muscle fibers without replicative capacity; however, satellite cells at the periphery of the myotubes persist as stem cells which are activated when myocytes are damaged.[2] Mature skeletal muscle expresses very little to no MyoD1 or myogenin, but are immunoreactive for desmin, a muscle-specific intermediate filament.[2]

In veterinary medicine, RMSs are typically diagnosed using histologic evaluation supplemented by desmin IHC staining; however, desmin is expressed in many canine neoplasms, including leiomyosarcomas, leiomyomas, and malignant fibrous histiocytomas, and, consequently, positive desmin immunoreactivity has a specificity of around 70% for RMS.[12] For this reason, when rhabdomyosarcoma is suspected, the current recommendation is to run an IHC panel consisting of desmin, MyoD1, and myogenin, all of which were positive in this tumor.[12]

Canine RMSs are subclassified into three broad categories: embryonal, alveolar, and pleomorphic. Embryonal RMSs are characterized by neoplastic cells that exhibit different stages of development, from myoblastic cells to myotubular cells. Embryonal RMSs are further divided into myotubular (multinucleated and elongated tubular cells), rhabdomyoblastic (large round cells with abundant cytoplasm), and spindle cell (fusiform cells arranged in streams) variants, depending on which embryonal features predominate.[2] Alveolar RMSs are further subclassified into classic alveolar RMS, where fibrous bands divide small round cells into clusters, and solid alveolar RMS, characterized by closely packed round cells with or without thin fibrous septa.[2] Finally, pleomorphic RMSs are characterized by haphazardly arranged spindle cells with marked anisocytosis and anisokaryosis with bizarre mitotic figures.[2] We agree with the contributor that the histologic features of this tumor most closely resembles a solid alveolar RMS. While histologic subtype carries prognostic significance in human RMSs, these associations have not yet been established in veterinary medicine.

Conference discussion focused on the various subtypes of rhabdomyosarcoma and the use of immunohistochemical stains (desmin, MyoD1, myogenin, and PTAH) used to diagnose them. The moderator drew attention to a subtype of embryonal rhabdomyosarcoma, the botryoid rhabdomyosarcoma, which most frequently occurs in the trigone of the urinary bladder in young, large breed dogs. Grossly, this tumor has a polypoid ("botryoid," or "grape-like") appearance that projects into the lumen of the urinary bladder. Histologically, this subtype contains undifferentiated myoblast cells and multinucleated myotube cells in a myxomatous stroma.

References:
1. Armeanu-Ebinger S, Bonin M, Häbig K, et al. Differential expression of invasion promoting genes in childhood rhabdomyosarcoma. *Int J Oncol*. 2011;38(4): 993–1000.
2. Caserto BG. A comparative review of canine and human rhabdomyosarcoma with emphasis on classification and pathogenesis. *Vet Pathol*. 2013;50(5): 806–826.
3. Cooper BJ, Valentine BA. Tumors of muscle. In: Meuten DJ, ed. *Tumors in Domestic Animals*, 5th ed. Ames, Iowa: Iowa State Press; 2017:444-466.
4. Gandi L, Vivekanand S. Maxillofacial rhabdomyosarcoma in the canine maxillofacial area. *Vet World*. 2012 5(9): 565-567.

5. Gillem JM, Sullivan L, Sorenmo KU. Diagnosis and multimodal treatment of metastatic maxillofacial juvenile embryonal rhabdomyosarcoma in a young golden retriever. *J Am Anim Hosp Assoc.* 2018:54(5)e545-05.

6. Hosoyama T, Aslam MI, Abraham J, et al. IL-4R drives dedifferentiation, mitogenesis, and metastasis in rhabdomyosarcoma. *Clin Cancer Res*. 2011;17(9): 2757–2766.

7. Kim DY, Hodgin EC, Cho DY, Varnado JE. Juvenile rhabdomyosarcomas in two dogs. *Vet Pathol.* 1996;33(4), 447-450.

8. Murakami M, Sakai H, Iwatani N, et al. Cytologic, histologic, and immunohistochemical features of maxillofacial alveolar rhabdomyosarcoma in a juvenile dog. *Vet Clin Pathol*. 2010;39(1):113–118.

9. Nakaichi M, Itamoto K, Hasegawa K. et al. Maxillofacial rhabdomyosarcoma in the canine maxillofacial area. *J Vet Med Sci.* 2007; 69(1):65-67.

10. Otrocka-Domagala I, Pazdzior-Czapula K, Gesek M, et al. Aggressive, solid variant of alveolar rhabdomyosarcoma with cutaneous involvement in a juvenile Labrador retriever. *J Comp Pathol.* 2015;152(2–3):177–181

11. Püsküllüoglu M, Lukasiewicz E, Miekus K, et al. Differential expression of Snail1 transcription factor and Snail1-related genes in alveolar and embryonal rhabdomyosarcoma subtypes. *Folia Histochem Cytobiol*. 2010;48(4):671–677.

12. Tuohy JL, Byer BJ, Royer S, et al. Evaluation of myogenin and MyoD1 as immunohistochemical markers of canine rhabdomyosarcoma. *Vet Pathol.* 2021; 58(3): 516-526.